

GSII

GSII-Preprint-96-40
August 1996

SEARCH FOR e^+e^- PAIRS WITH NARROW SUM-ENERGY DISTRIBUTIONS IN HEAVY-ION COLLISIONS

The EPoS II collaboration :

R. GANZ, R. BÄR, A. BALANDA, J. BAUMANN, W. BERG, K. BETHGE,
A. BILLMEIER, H. BOKEMEYER, H. FEHLHABER, H. FOLGER,
J. FORYCIAR, O. FRÖHLICH, O. HARTUNG, M. RHEIN, M. SAMEK,
P. SALABURA, W. SCHÖN, D. SCHWALM, K.E. STIEBING, P. THEE

SCAN-9609029



CERN LIBRARIES, GENEVA

Gesellschaft für Schwerionenforschung mbH
Planckstraße 1 • D-64291 Darmstadt • Germany
Postfach 110552 • D-64220 Darmstadt • Germany

Search for e^+e^- pairs with narrow sum-energy distributions in heavy-ion collisions*

The EPoS II collaboration

R. Ganz², R. Bär³, A. Balanda⁴, J. Baumann^{1,2}, W. Berg³, K. Bethge³, A. Billmeier³,
H. Bokemeyer¹, H. Fehlhaber³, H. Folger¹, J. Foryciar^{1,4}, O. Fröhlich³,
O. Hartung³, M. Rhein¹, M. Samek^{2,4}, P. Salabura^{1,4}, W. Schön³, D. Schwalm^{2,5},
K.E. Stiebing³, and P. Thee³

¹ Gesellschaft für Schwerionenforschung, D-64291 Darmstadt, FRG

² Physikalisches Institut Univ. Heidelberg, D-69120 Heidelberg, FRG

³ Institut für Kernphysik Univ. Frankfurt, D-60486 Frankfurt a.M., FRG

⁴ Jagiellonian Univ. Krakow, PL 30-059 Krakow, PL

⁵ Max Planck Institut für Kernphysik, D-69117 Heidelberg, FRG

Abstract:

The investigation of e^+e^- pairs emitted in heavy-ion collisions at the Coulomb barrier has been continued at GSI Darmstadt with the redesigned spectrometer EPoS II. Due to its enlarged efficiency for the detection of e^+e^- pairs the reproducibility of the narrow line structures previously observed in the e^+e^- sum-energy spectra with the EPOS I spectrometer could be tested using a highly improved statistical databasis. No lines have been observed with the new data sets when applying the same selection criteria as in the old data. Our measurements give upper limits for the cross-sections of these lines, which are a factor of up to 10 smaller than the cross-sections deduced from the EPOS I data.

1. Introduction

The observation [1,2,3] of e^+e^- pairs with narrow sum-energy distributions in heavy-ion collisions has caused extensive experimental and theoretical activities. We report in the present letter on a series of measurements carried out at the UNILAC of the GSI in Darmstadt with the new Electron-Positron Solenoid spectrometer EPoS II to reinvestigate the two collision systems $^{238}\text{U}+^{181}\text{Ta}$ and $^{238}\text{U}+^{232}\text{Th}$, where in previous experiments with the EPOS I set-up several narrow line structures were identified in the e^+e^- sum-energy spectra in coincidence with both scattered ions [1,2]. The most striking feature of these sum-energy lines, which were observed in the laboratory system without correcting for kinematical shifts, is their narrow width of less than 40 keV. Moreover, the occurrence of the lines appeared to be restricted to narrow beam-energy regions, and the signals could be enhanced over the continuous spectra, caused by atomic and nuclear processes, in subsets of the data obtained by selecting on the energy sharing between

the positron and the electron and furthermore on the arrival times of the two leptons at the detectors, which measure - if they are emitted promptly at the target - their flight times and thus their emission angles with respect to the solenoid axis.

The present reinvestigation became necessary as no convincing hypothesis has yet been put forward which is able to explain the origin of these lines (see e.g. [4]). In particular, explanations based on the two-body decay of hitherto unknown particles had to be dismissed due to the results of these investigations; indeed, in our last experimental campaign with EPOS I, which was tailored to investigate the particle hypothesis, the back-to-back emission characteristic of the two leptons expected in this case could not be proven to be a general feature of the lines [2]. In the absence of any physics-based justification for the above mentioned restrictions and cuts in the experimental parameter space, however, the statistical relevance of the lines has to be reconsidered and their reproducibility becomes the key issue. We therefore decided to redesign the EPOS spectrometer in order to increase the e^+e^- coincidence efficiency and to enlarge the coverage of the parameter space subtended by the spectrometer, with the aim to reproduce the narrow e^+e^- sum-energy lines on a greatly improved statistical databasis and to study in more detail some of their properties, in particular the angular correlation between the two leptons and the beam-energy and emission-angle dependences.

Similar attempts to reproduce the results of EPOS I have been pursued at Argonne National Laboratory by the APEX collaboration [5,6]. Moreover, the ORANGE collaboration at GSI has recently reinvestigated some of their previous results quoted in ref.[3].

2. The EPoS II spectrometer

As EPOS I [7], the redesigned EPoS II spectrometer (see fig.1 and ref. [8]) is based on a solenoidal magnetic transport system perpendicular to the beam axis, which allows to place the high-resolution lepton-detection system far away from the radiation-loaded region in the vicinity of the target. To distinguish positrons from electrons the new device again utilizes the orientation of the helical trajectories of the leptons in the magnetic field, but now avoids any material along the transportation path of the leptons. The lepton-detection system consists of four sets of Si(Li) detectors, each of which is build out of two planar detectors mounted back-to-back. They are placed parallel to the solenoid axis in both arms of the spectrometer. From geometric considerations it is obvious that electrons emitted from the target will always hit one side and positrons the opposite side of such a detector sandwich (see inlay of fig.1). The lepton-detection system in both spectrometer arms is in addition surrounded by rings consisting out of 24 NaI-scintillator crystals each to further identify positrons via their 511 keV annihilation radiation. The enormous flux of δ -electrons at low kinetic energies E_{e^-} is suppressed by displacing the detectors from the solenoid axis by 17 mm; thus leptons with energies $E_{e^-} < 110$ keV cannot hit the detector because of their smaller gyration radii in the magnetic guiding field of $B \approx 1.2$ T. Due to this geometry all mechanical baffles used in the EPOS I spectrometer could be avoided in the new set-up. In addition, a new target design was employed to minimize the amount of material next to the beam spot.

A further advantage of the new set-up is that electrons and positrons can be detected in both arms of the spectrometer and that the four detectors allow to clearly distinguish for both types of leptons four solid-angle ranges of lepton-emission directions (forward/backward and left/right with respect to the beam axis). Furthermore, each combination of an electron with a positron detector now covers an e^+e^- opening-angle range which can be attributed to one of four overlapping bins $\langle\Theta_{e^+e^-}\rangle$ with mean values around $\Theta_{e^+e^-} = 20^\circ, 60^\circ, 120^\circ$ and 160° .

For e^+e^- pairs with a given sum energy $E_\Sigma = E_{e^+} + E_{e^-}$ the detection efficiency essentially depends on the opening-angle characteristics and the difference energy distribution $E_\Delta = E_{e^+} - E_{e^-}$. With the new set-up we reach a full-energy pair-detection efficiency including the detection of at least one 511 keV annihilation γ in the NaI-ring of $\varepsilon_{is}'' = 5.1\%$ for isotropically emitted leptons with $E_\Sigma = 800$ keV and $E_\Delta = 0$ keV. This exceeds the corresponding (average) value $\varepsilon_{is}' = 0.7\%$ of EPOS I by a factor of 7. Even for back-to-back emitted leptons, for which the pair-detection efficiency of EPOS I was optimized and reached a maximum of $\varepsilon_{bb}' = 1.7\%$ ($E_\Sigma = 800$ keV, $E_\Delta = 0$ keV), we still gain a factor of more than 5 in efficiency with the new spectrometer, i.e. $\varepsilon_{bb}'' = 9.2\%$. In addition, the new heavy-ion detection system now covers an azimuthal angle of almost 2π around the beam axis, which results in another 30% gain of detection efficiency as compared to EPOS I; note that the detection of both scattered heavy ions is required in all measurements. A more detailed description of the new spectrometer EPoS II will be presented in ref. [8].

The performance of EPoS II has been thoroughly tested in source measurements. In particular the ^{90}Sr -source, which emits monoenergetic e^+e^- pairs ($E_\Sigma = 739$ keV) due to an Internal Pair Conversion (IPC) process of an E0 transition of 1761 keV, is an excellent probe to study the performance of the spectrometer under conditions similar to those encountered in in-beam experiments with regard to the intense δ -electron background; for the ^{90}Sr -source the pair-creation process is immersed in an overwhelming electron background of five orders of magnitude higher yield from the main β -decay branch. The results of these measurements are found to be in quantitative agreement with Monte-Carlo simulations [9]. The resolution achieved for the e^+e^- sum-energy line at $E_\Sigma = 739$ keV is 17 keV (FWHM).

To check the in-beam performance of the spectrometer in more detail a ^{206}Pb target has been bombarded with 5.82 MeV/u ^{238}U ions. Due to Coulomb excitation a 3^- state is populated in ^{206}Pb [10], which decays to the first excited 2^+ state either by an E1 γ -transition of 1844 keV or by an E1-IPC. Correcting for the shifts of the leptons due to their emission from the recoiling ^{206}Pb -nuclei, a e^+e^- sum-energy line is observed [9] with an intensity, which agrees with the value deduced from the yield of the corresponding γ -line detected with the Ge-detector using conversion coefficients given in ref. [11].

3. Experiments and Results

The experiments with the new EPoS II spectrometer performed so far were devoted to the reinvestigation of the U+Ta and U+Th collision systems and the question of the reproducibility of the e^+e^- sum-energy lines reported by EPOS I [1,2]. Therefore special care was taken to subtend as closely as possible the beam energy range investigated by EPOS I.

The $^{238}\text{U}+^{181}\text{Ta}$ measurements were carried out at U-beam energies of 5.92, 5.96, 5.98, 5.99, 6.00 and 6.06 MeV/u, thereby covering the energy region where the sum-energy line at $E_{\Sigma} = 748 \pm 8$ keV ($\delta E_{\Sigma} = 33$ keV FWHM) has been observed as reported in ref. [2]. Furthermore, an experiment has been performed at 6.30 MeV/u in order to reproduce the sum-energy lines observed at $E_{\Sigma} = 625 \pm 8$ keV ($\delta E_{\Sigma} = 20$ keV FWHM) and $E_{\Sigma} = 805 \pm 8$ keV ($\delta E_{\Sigma} = 27$ keV FWHM) [2]. The $^{238}\text{U}+^{232}\text{Th}$ system was investigated at U-beam energies of 5.68, 5.83, 5.85, 5.87, 5.91 and 5.95 MeV/u. For this system sum-energy lines were found by EPOS I at $E_{\Sigma} = 608 \pm 8$ keV ($\delta E_{\Sigma} = 25$ keV FWHM) and $E_{\Sigma} = 809 \pm 8$ keV ($\delta E_{\Sigma} = 40$ keV FWHM) when selecting beam energies between 5.85 - 5.90 MeV/u and 5.87-5.90 MeV/u, respectively [2]. Moreover, at a beam energy of 5.83 MeV/u the observation of a sum-energy line at $E_{\Sigma} = 760 \pm 20$ keV was reported in [1]. In the EPoS II as well as in the EPOS I measurements the incident beam energy was checked regularly by time-of-flight measurements over a distance of 11 m; the absolute beam-energy determination is estimated to be better than 0.02 MeV/u.

Refined target production procedures allowed to use rolled metallic Thorium targets of $470 \mu\text{g}/\text{cm}^2$, which led to a beam-energy loss of 0.10 MeV/u. In contrast, in EPOS I ThF_4 targets of $280 \mu\text{g}/\text{cm}^2$ (sandwiched between $20 \mu\text{g}/\text{cm}^2$ and $5 \mu\text{g}/\text{cm}^2$ C-foils) have been employed, which resulted, however, in similar beam-energy losses of 0.08 MeV/u. The thickness of the Tantalum targets were $370 \mu\text{g}/\text{cm}^2$ as compared to $400 \mu\text{g}/\text{cm}^2$ ($600 \mu\text{g}/\text{cm}^2$ for a run at 6.16 MeV/u) used in the EPOS I measurements, which resulted again in similar energy losses of the projectile in the target of 0.09 MeV/u as compared to 0.10 MeV/u (0.14 MeV/u). All measurements were performed as in EPOS I at beam currents of 1-2 pA. During four beam times about $5.0 \cdot 10^5$ e^+e^- events were recorded in coincidence with both scattered heavy ions for each of the two systems, which presents a gain of a factor of 10 (U+Th) and 25 (U+Ta), respectively, compared to the EPOS I data.

In order to reproduce the line structures observed in the previous experiments we first restricted in the off-line analysis the parameter space spanned in the new measurements with respect to (a) the U-beam energy and (b) to the energy sharing between the electron and the positron, summing over beam energies and applying wedge cuts identical to those found to enhance the respective line structures in the EPOS I data (see table I); we omitted the selection on the time-of-flight of the leptons, used in EPOS I to enhance the signal-to-background ratio, as it affects the efficiencies of the two set-ups in a rather complicated and scenario-dependent way. The two cuts (a) and (b) should be sufficient as the lines were already observable under these conditions in the EPOS I

data. Therefore, the increased number of pairs collected with the new spectrometer should lead already in these data subsets in statistically significant structures.

All e^+e^- sum-energy spectra obtained with EPoS II using the two selection criteria discussed above were found to be smooth and well represented by distributions generated by event mixing; in particular, no evidence for narrow line structures at sum-energies given by the EPOS I measurement has been observed. Fig. 2 displays the resulting EPoS II spectra applying the two conditions (a) and (b) associated with the three most prominent lines of EPOS I, the 608 and 809 keV lines in the U+Th and the 748 keV line in the U+Ta system (see also table I).

When comparing EPOS I and EPoS II measurements one has to be aware that the properties of the e^+e^- pairs leading to the line structures observed in EPOS I, in particular their angular correlation with respect to the heavy ions and the opening-angle distribution of the two leptons, are not known in detail. Therefore we will assume two rather contrary lepton-emission scenarios to estimate the size of the lines expected in the spectra shown in fig. 2.

We first calculate the expected intensities from the cross section derived for the EPOS I lines under the following assumptions: (i) The line cross-sections per solid angle in the center-of-mass of the two heavy ions are obtained by averaging over the heavy-ion scattering angles with $44^\circ \leq \Theta_{cm} \leq 140^\circ$ for the $^{238}\text{U} + ^{181}\text{Ta}$ system and $41^\circ \leq \Theta_{cm} \leq 140^\circ$ for the $^{238}\text{U} + ^{232}\text{Th}$ system, respectively, which is the angular range covered by the coincident heavy-ions detectors in both set-ups. (ii). The line cross-sections are constant within the beam energy range spanned by the selected U-beam energies and the energy loss in the target and (iii) do not depend on the orientation of the scattering plane with respect to the solenoid axis. (iv) The emission of the leptons contributing to the sum-energy lines takes place at the intersection of the solenoid axis with the beam axis where also the targets are located. (v) The kinetic energy of the e^+e^- pair is shared by the two leptons according to the ranges allowed by the wedge cuts in the $E_{e^+} - E_{e^-}$ plane (see table I). (vi) The emission directions of both leptons contributing to the sum-energy lines are isotropically distributed in the heavy-ion c.m. system, which implies, that also the opening angle distribution of the two leptons is isotropic. The cross-sections deduced under these assumptions - referred to as the 'isotropic' scenario in this letter - from the yields of the line structures observed in the EPOS I measurements [2] are given in table I.

By taking into account the detection efficiencies of EPoS II appropriate for the 'isotropic' scenario we have calculated from these cross-sections the line yields we should expect to observe in our new measurements. As indicated in the right column of fig. 2, where the differences between the measured sum-energy spectra and the normalized event-mixing distributions are displayed, the expected line yields are clearly in contradiction with the new high-statistics data. In table I these discrepancies are quantified by quoting the upper cross-section limits derived from the e^+e^- sum-energy distributions for the beam energies and wedge cuts as specified. These limits are 2σ limits for the occurrence of lines with positions and widths as reported by EPOS I, using the event-mixing distributions as background spectra and the procedure described in ref. [12]. The deduced limits are significantly below the corresponding cross-sections

obtained for the EPOS I line structures within the 'isotropic' scenario.

When changing the scenario the cross-sections derived for the EPOS I lines as well as the cross-section limits deduced from the EPoS II experiments will change because of the scenario dependence of the detection efficiencies of the two set-ups. However, the yields of the line structures expected in the new measurements will be much less affected by such a change as the parameter space covered in the new experiments includes to a great extent that of the EPOS I measurements. A special case rather contrary to the isotropic opening angle distribution of the two leptons assumed above is the 'back-to-back' scenario, where the positrons and electrons contributing to the sum-energy line are assumed to have a 180° correlation. This scenario was originally motivated by the particle hypothesis: Indeed, for particles, which are produced isotropically with small kinetic energies (<50 keV) in the heavy-ion cm-system and decay freely into an electron-positron pair, the decay pattern results in an approximate back-to-back correlation as well as in a narrow sum-energy line and in an energy sharing, causing a symmetric distribution around $E_{e^+} = E_e$. [13].

As discussed in ref. [2] the 809 keV line observed by EPOS I in the U+Th system was found to be qualitatively consistent with a 'back-to-back' scenario. To be again specific, for the 'back-to-back' scenario all suppositions of the 'isotropic' one are kept with the exception of (vi), which is replaced by the assumption that, while the electron of the pair is still isotropically distributed in the heavy-ion cm-system, the positron is emitted in the opposite direction of the electron. Using the appropriate efficiencies the yield of the 809 keV lines observed by EPOS I then results in a cross-section of $d\sigma/d\Omega_{cm} \approx 1.3 \mu\text{b/sr}$, which is a factor of 2.4 smaller than the isotropic cross-section since EPOS I was optimized for the investigation of the particle hypothesis. On the other hand, since the EPoS II efficiency is also enhanced for the 'back-to-back' scenario, the yield of the 809 keV line expected in the new measurement shown in the middle panel of fig. 2 is only 20% smaller than for the 'isotropic' assumption, still leaving us with a pronounced discrepancy between the expected line yield and the smoothness of the observed spectrum.

For the 'back-to-back' scenario, however, the sensitivity of the new measurements can be even further increased by utilizing the property of EPoS II to distinguish between different opening angles of the two coincident leptons. Restricting the EPoS II data analysis to e^+e^- pairs, which have been recorded by detector combinations corresponding to the $<160^\circ>$ opening-angle region (which includes 180°), the total number of pairs is reduced by about a factor of 4. The resulting sum-energy distribution, relevant for the 809 keV line observed by EPOS I in the U+Th system, is shown in fig. 3 together with the expected line yield. Again, no corresponding line is observed in the new data and a 2σ cross-section limit of $0.09 \mu\text{b/sr}$ can be deduced within this scenario for a line at this sum-energy with an expected width of 40 keV (FWHM).

Although the 'back-to-back' correlation could not be proven to be a general property of the sum-energy lines [2], table I contains the cross-sections calculated from the yield of all the lines observed by EPOS I within the 'back-to-back' scenario and compares them with the corresponding cross-section limits deduced from the EPoS II $<160^\circ>$ -spectra, none of which show evidence for line structures. All resulting cross-section

limits are about a factor of 10 smaller than the EPOS I values.

A strong beam-energy dependence of the line-production cross-sections was suggested by the EPOS I results. In particular, the occurrence of the 608 and 809 keV lines in the U + Th system appeared to be connected with sharp thresholds or even resonances within narrow bombarding-energy ranges between 5.85-5.90 MeV/u and 5.87-5.90 MeV/u, respectively. Although the finite target thickness is equivalent to a 0.10 MeV/u wide beam-energy interval we have performed our measurements at several beam energies to closely cover the relevant projectile-energy region. None of the resulting sum-energy spectra showed any statistically significant line. The cross-section limits derived for the U + Th system as a function of the U-beam energy are compiled in table II; note that even these individual limits are significantly smaller than the EPOS I cross-sections.

A variety of additional analyses have been carried out on the data collected with EPoS II. For example, in one of these approaches we limited the e^+e^- opening angles to the two bins $<60^\circ>$ and $<160^\circ>$ and the orientation angle Φ of the heavy-ion scattering plane with respect to the solenoid axis to $25^\circ \leq \Phi \leq 155^\circ$ in order to imitate even closer the coverage of the parameter space in the EPOS I experiment. Again we did not observe any relevant line structures, although the decreasing efficiency caused by additional cuts is leading to spectra with increasing fluctuations around the smooth event-mixing distributions; thus a line-like 2σ -fluctuation appeared around 610 keV in the sum-energy spectrum for U + Th obtained with the above windows and a wedge cut relevant for the 608 keV line, which - besides of being statistically not relevant - exhausts only 20% of the expected line intensity.

In summary, all our attempts led to the same result: We did not succeed in reproducing with our statistically improved data basis the e^+e^- sum-energy lines reported by EPOS I [1,2].

4. Discussion

The obvious discrepancy between the outcome of our new experiments and the findings of EPOS I does require some discussion of possible causes of this unexpected result, in particular, as this discrepancy is also corroborated by the APEX collaboration [5]. APEX derived similar upper limits as EPoS II for the cross-section of narrow lines in the e^+e^- sum-energy spectra following $^{238}\text{U} + ^{232}\text{Th}$ and $^{238}\text{U} + ^{181}\text{Ta}$ collisions, although the sensitivity of the APEX experiments with regard to the question of reproducibility of the EPOS I lines is less stringent if one allows for a narrow beam-energy dependence of the line cross-section [6].

As already pointed out, in the present experiment we have tried to repeat the previous EPOS I measurements as closely as possible. In particular, the energy loss of the projectiles in the targets were similar in both experiments and even possible deteriorations of the targets during the measurements are unlikely to be responsible for our failure to reproduce the lines as the targets have been changed frequently and the new experiments were carried out at several beam energies subtending the relevant

region. Moreover, the enlarged coverage by EPoS II of the opening angles $\Theta_{e^+e^-}$ of the two leptons and of the orientation of the heavy-ion scattering plane with respect to the solenoid axis, which might not add to the signal, is also unlikely to cause the discrepancy as shown by the analysis discussed above, in which the EPOS I acceptance for these parameters was imitated. As supported by extensive Monte-Carlo simulations, the only remaining difference in the acceptance of the two set-ups is that EPoS II - in contrary to EPOS I - cannot detect leptons emitted close to 90° with respect to the beam axis, which is due to the particular off-axis arrangement of the lepton detectors in EPoS II. However, not only is it difficult to imagine a scenario which would result in such a narrow, disk-like emission pattern of the leptons perpendicular to the beam directions, this loophole also seems to be unlikely in view of a recent APEX result: The APEX spectrometer [14] allows to select these special lepton-emission angles, which results in a strongly increased sensitivity for this scenario, in particular as one has to assume in this case that the EPOS I line yields are located at these lepton angles; a corresponding investigation of the APEX data did not show evidence for this allegation [15].

Accepting the conclusion that our failure to reproduce the sum-energy lines is not caused by differences in the acceptance of EPoS II as compared to EPOS I or by some unknown and therefore uncontrolled parameter in the experiment, and accepting that the EPOS I lines - as shown by extensive Monte Carlo Simulations - are not due to background processes caused e.g. by the various baffles used in EPOS I but avoided in EPoS II, the statistical significance of the e^+e^- lines observed in the previous experiments remains to be discussed. In fact, the absence of a physical justification of the analysis windows necessary to increase the signal-to-background ratio of the lines was the prime motivation questioning their reproducibility.

The problem of judging the statistical significance of line structures enhanced by cuts is readily illustrated by two examples: The first one concerns the narrow sum-energy line around 740 keV ($\langle E_\Sigma \rangle = 723 \pm 10$ keV using the final calibration) observed in the first $^{238}\text{U} + ^{181}\text{Ta}$ run performed with EPoS II [9] in order to reproduce the 748 keV line. The 723 keV line was only weakly visible in the total e^+e^- sum-energy spectrum but clearly seen (with a nominal significance of 5σ) when requiring cuts with respect to E_Δ and the scattering angles of the heavy ions. However, not only was the energy of the line at variance with the previous value of 748 keV, also two follow-up, high-statistic experiments performed with an unchanged EPoS II set-up failed to reproduce the line. The second example comes from an investigation suggested in ref. [16] where we took advantage of the enlarged data basis collected in the EPoS II experiment. We randomly distributed - on an event-by-event basis - the e^+e^- pairs collected at a certain beam energy into two subsets. While one of these subsets was kept as a reference sample, we searched for narrow line structure in the other subset by choosing different E_Δ - and time-of-flight cuts. Surprisingly enough, we were able to find a cut - leading to a spectrum of similar statistics as in a typical EPOS I experiment -, which enhances a 2σ -structure visible at 655 keV in the initial subset to a line of $\approx 5\sigma$, which is comparable in width and intensity to those observed with EPOS I. However, applying the identical cut to the reference sample the resulting spectrum does not show any line structure at this energy.

Both examples underline that the statistical significance of spectra obtained by introducing selection criteria, which are acceptable when looking for something unexpected but which cannot be supported later by a coherent physical picture, has to be taken with great precautions. In this situation an independent reproduction based on a considerably larger data set is the only way to confirm the existence of a physical effect. Since we failed to demonstrate the reproducibility of the lines observed by EPOS I and derived cross-section limits which are a factor of up to 10 smaller than the values implied by the previous results, the physical relevance of the EPOS I lines is questionable.

References

* Supported by BMBF # 06 HD 525I and # 06 OF 463, NATO CRG #910990, and EG # ERBCIPD-CT 94-0091

- [1] T.E. Cowan, H. Backe, K. Bethge, H. Bokemeyer, H. Folger, J.S. Greenberg, K.Sakaguchi, D. Schwalm, J. Schweppe, K.E. Stiebing and P. Vincent, Phys.Rev. Lett. 56 (1986) 444
- [2] P. Salabura, H. Backe, K. Bethge, H. Bokemeyer, T.E. Cowan, H. Folger, J.S. Greenberg, K. Sakaguchi, D. Schwalm, J. Schweppe and K.E. Stiebing, Phys. Lett B 245 (1990) 153
- [3] I. Koenig, E. Berdermann, F. Bosch, W. Koenig, P. Kienle, C.Kozhuharov, A. Schröter, and H. Tsertos, Z. Phys. A 346 (1993) 153, and references therein
- [4] B. Müller, in: Atomic physics of highly ionized atoms, ed. R. Marrus (Plenum, New York, 1989) p. 39; A. Schäfer, J. Phys. G 15 (1989) 373
- [5] I. Ahmad et al., Phys. Rev. Lett. 75 (1995) 2658
- [6] T.E. Cowan and J.S. Greenberg, Phys. Rev. Lett., to be published
I. Ahmad et al., Phys. Rev. Lett., to be published
- [7] H. Bokemeyer et al. in : Physics of strong fields, ed. W. Greiner, NASI Series B (Plenum, New York, 1987) p. 195
- [8] M. Samek et al., to be published
- [9] R. Bär et al., Nucl. Phys. A 583 (1995) 237
- [10] G. Eckert et al., Z. Phys. A 343 (1992) 267
- [11] P. Schlüter et al., Phys. Rep. 75 (1981) 327
- [12] Review of Particle Properties, Phys. Rev. D45 (1992), part II
- [13] T.E. Cowan, S. Greenberg et al. in: Physics of strong fields, ed. W. Greiner, NASI Series B (Plenum, New York, 1987) p. 111
- [14] I. Ahmad et al., NIM A 370 (1996) 539
- [15] F.L.H. Wolfs (APEX), priv. communication
- [16] B.P. Roe, Probability and Statistics in Experimental Physics (Springer, Berlin-Heidelberg-New York, 1992)

Figure Captions

Fig1: Schematic view of the new Electron Positron Spectrometer EPoS II. The apparatus is embedded in a solenoidal magnetic field B produced by pancake-like coils (not shown). Insert: Cross section through the Si(Li) - and NaI - detector arrays.

Fig2: The left column displays the measured e^+e^- sum-energy spectra obtained for the same U-beam energies and wedge cuts used in EPOS I to enhance the lines. The solid curve was generated by event mixing and normalized to the total number of counts in the spectrum. The right column displays the differences between the experimental spectra and the event-mixing curves together with the lines expected from the EPOS I measurements assuming the 'isotropic' scenario. Upper panels: $^{238}\text{U} + ^{232}\text{Th}$ system, 608 keV line. Middle panels: $^{238}\text{U} + ^{232}\text{Th}$ system, 809 keV line. Lower panels: $^{238}\text{U} + ^{181}\text{Ta}$ system, 748 keV line.

Fig3: Same spectra as shown in the middle panel of fig. 2 but restricting in addition the opening angle between the two leptons to the $<160^\circ>$ bin. The thin line in the right panel is the expected yield of the 809 keV line observed by EPOS I assuming the 'back-to-back' scenario.

Table I
Comparison of the EPOS II cross-section limits for narrow sum-energy lines with the results of EPOS I

| Sum-energy Lines ⁿ⁾ | | | EPOS I ^{a)} | | EPOS II | | | | |
|--------------------------------|------------------------------------|----------------------------------|--|---------------------------|---|--|---------------------------|---|--|
| HI System | $\langle E_{\Sigma} \rangle$ [keV] | δE_{Σ} (FWHM) [keV] | Wedge cut ^{c)} | E_{Beam} [MeV/u] | $\frac{d\sigma(\text{iso})^{d)}$ $d\Omega_{\text{cm}}$ [$\mu\text{b}/\text{sr}$] | $\frac{d\sigma(\text{bb})^{e,f)}$ $d\Omega_{\text{cm}}$ [$\mu\text{b}/\text{sr}$] | E_{Beam} [MeV/u] | $\frac{d\sigma(\text{iso})^{d,g)}$ $d\Omega_{\text{cm}}$ [$\mu\text{b}/\text{sr}$] | $\frac{d\sigma(\text{bb})^{e,h)}$ $d\Omega_{\text{cm}}$ [$\mu\text{b}/\text{sr}$] |
| | 625±8 | 20 | 0.57E ₊ <E ₋ <1.64E ₊ | 6.24,6.30, 6.38 | 3.2±0.8 | 1.3±0.3 | 6.30 | <0.4 | <0.13 |
| U+Ta | 748±8 | 33 | 0.14E ₊ <E ₋ <1.50E ₊ | 5.93,5.98 6.03,6.16 | 5.7±1.3 | 2.3±0.5 | 5.96,5.98 5.99,6.06 | <0.3 | <0.03 |
| | 805±8 | 27 | 0.34E ₊ <E ₋ <1.64E ₊ | 6.24,6.30 6.38 | 3.3±0.8 | 1.4±0.4 | 6.30 | <0.8 | <0.15 |
| | 608±8 | 25 | 0.67E ₊ <E ₋ <1.50E ₊ | 5.85,5.87 5.88,5.90 | 2.7±0.6 | 1.1±0.3 | 5.85,5.87 5.91 | <0.3 | <0.15 |
| U+Th | 760±20 ^{b)} | ≤80 | 0.75E ₊ <E ₋ <1.25E ₊ | 5.83 | - | - | 5.83 | <0.9 ^{g)} | <0.27 ^{h)} |
| | 809±8 | 40 | 0.68E ₊ <E ₋ <1.25E ₊ | 5.87,5.88 5.90 | 3.1±0.7 | 1.3±0.3 | 5.87,5.91 | <0.4 | <0.09 |

a) from ref.[2] with the exception of b)

b) from ref.[1]

c) kinetic energy sharing between electron (E₋) and positron (E₊)

d) isotropic scenario (see text)

e) back-to-back-scenario (see text)

f) 2 σ -limits

g) assuming $\delta E_{\Sigma} = 40$ keV

Table II

EPOS II cross-section limits for a 608 keV and 809 keV sum-energy line in the $^{238}\text{U} + ^{232}\text{Th}$ system as a function of the U-beam energy

| $E_{\text{beam}}^{\text{a}}$ [MeV/u] | $\langle E_{\Sigma} \rangle = 608 \text{ keV}$ | | $\langle E_{\Sigma} \rangle = 809 \text{ keV}$ | | | |
|---|--|-----------------------------------|--|---|--|---|
| | $0.67 E_{e+} < E_e < 1.50 E_{e+}$ | $0.68 E_{e+} < E_e < 1.25 E_{e+}$ | $d\sigma(\text{iso})^{\text{c,e}}$ $d\Omega_{\text{cm}}$ [$\mu\text{b}/\text{sr}$] | $d\sigma(\text{bb})^{\text{d,e}}$ $d\Omega_{\text{cm}}$ [$\mu\text{b}/\text{sr}$] | $d\sigma(\text{iso})^{\text{c,e}}$ $d\Omega_{\text{cm}}$ [$\mu\text{b}/\text{sr}$] | $d\sigma(\text{bb})^{\text{d,e}}$ $d\Omega_{\text{cm}}$ [$\mu\text{b}/\text{sr}$] |
| 5.95 | < 0.5 | < 0.14 | < 0.5 | < 0.13 | < 0.5 | < 0.13 |
| 5.91 | < 0.7 | < 0.19 | < 0.7 | < 0.18 | < 0.7 | < 0.18 |
| 5.87 | < 0.6 | < 0.30 | < 0.5 | < 0.14 | < 0.5 | < 0.14 |
| 5.85 ^{-b)} | < 0.7 | < 0.19 | < 0.7 | < 0.18 | < 0.7 | < 0.18 |
| 5.83 | < 0.6 | < 0.19 | < 0.6 | < 0.18 | < 0.6 | < 0.18 |
| 5.68 | < 0.5 | < 0.13 | < 0.4 | < 0.12 | < 0.4 | < 0.12 |

- a) The energy loss in the target amounts to 0.10 MeV/u
- b) After transversing a C-backing of 0.06 MeV/u
- c) isotopic scenario (see text)
- d) back-to-back scenario (see text)
- e) 2σ -limits assuming a FWHM of $\delta E_{\Sigma} = 25 \text{ keV}$ (40 keV) for the 608 keV (809 keV) line

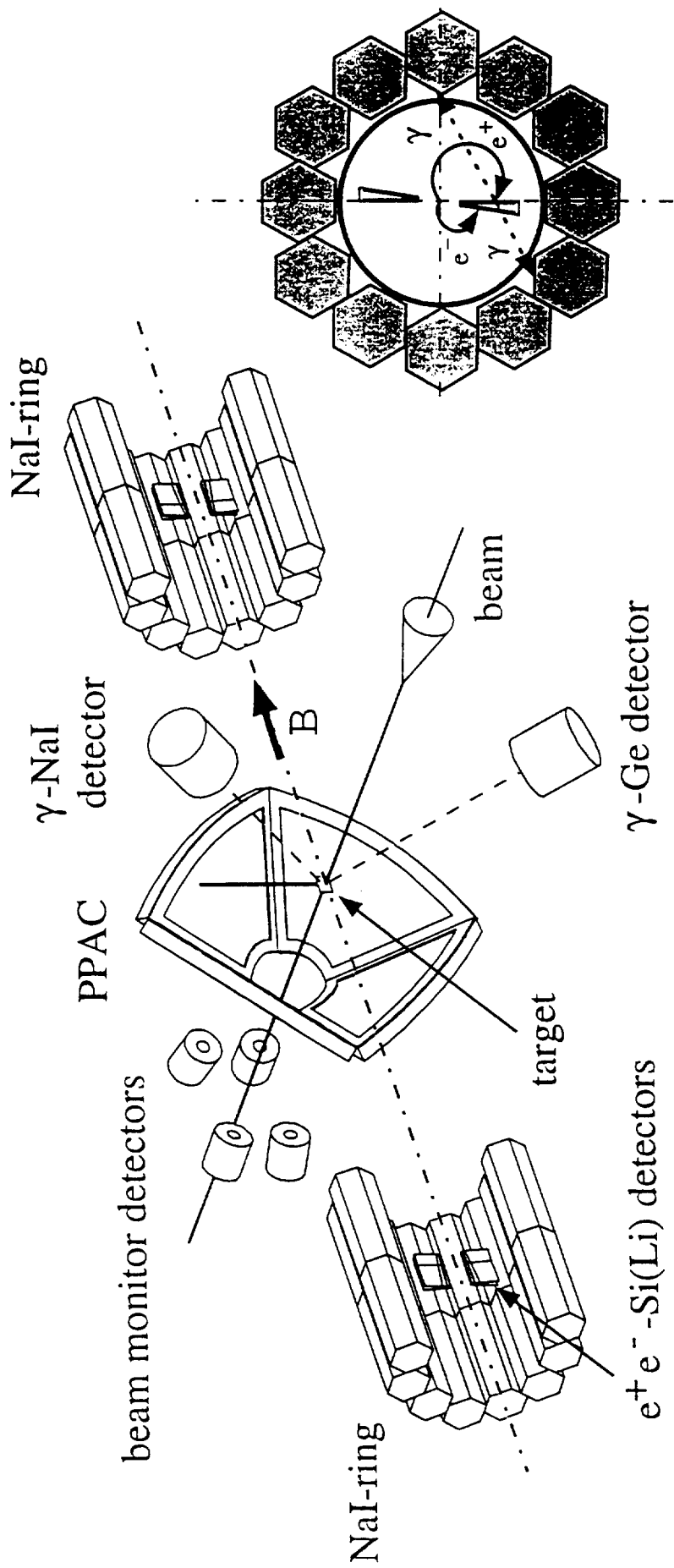


Figure 1:

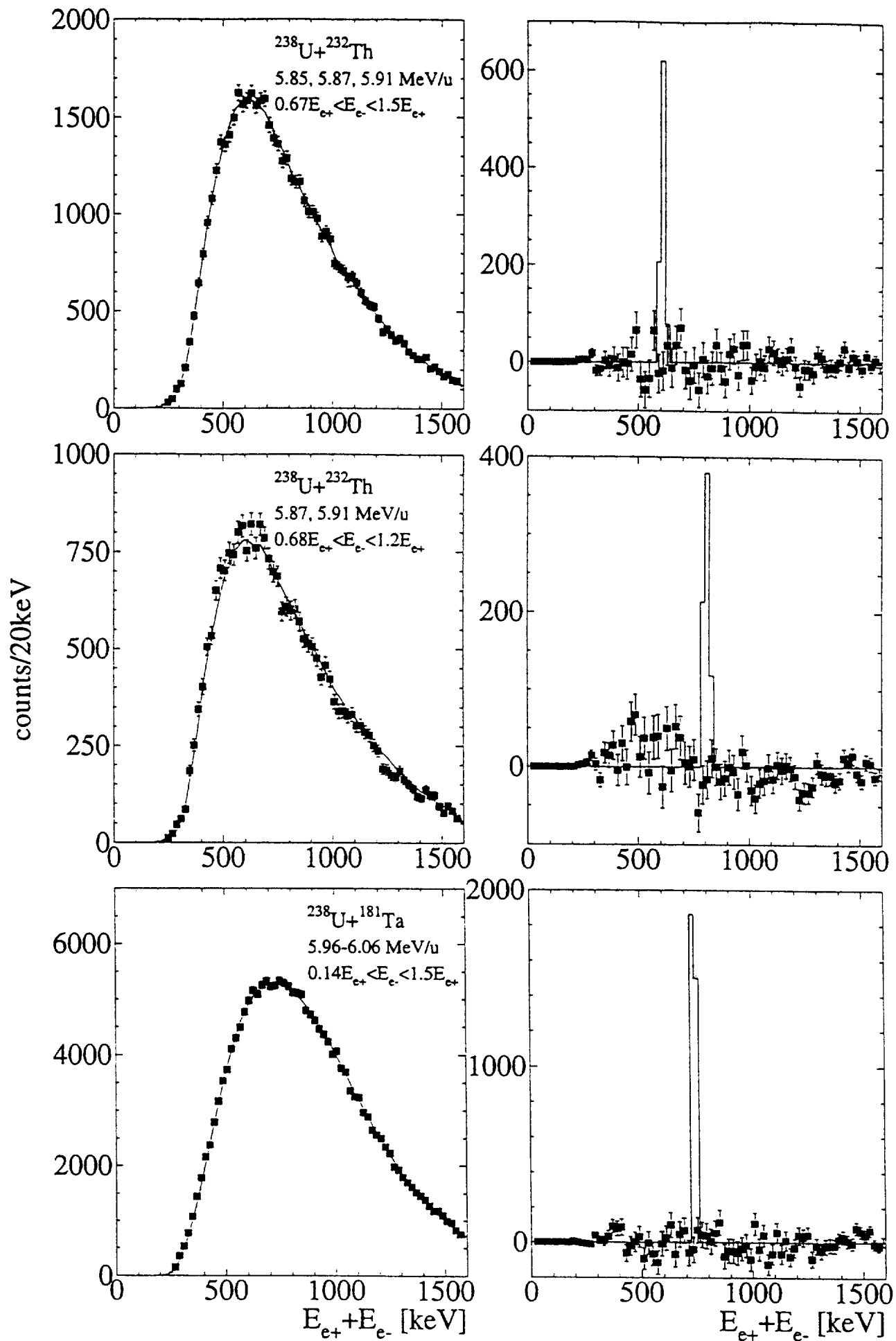


Figure 2:

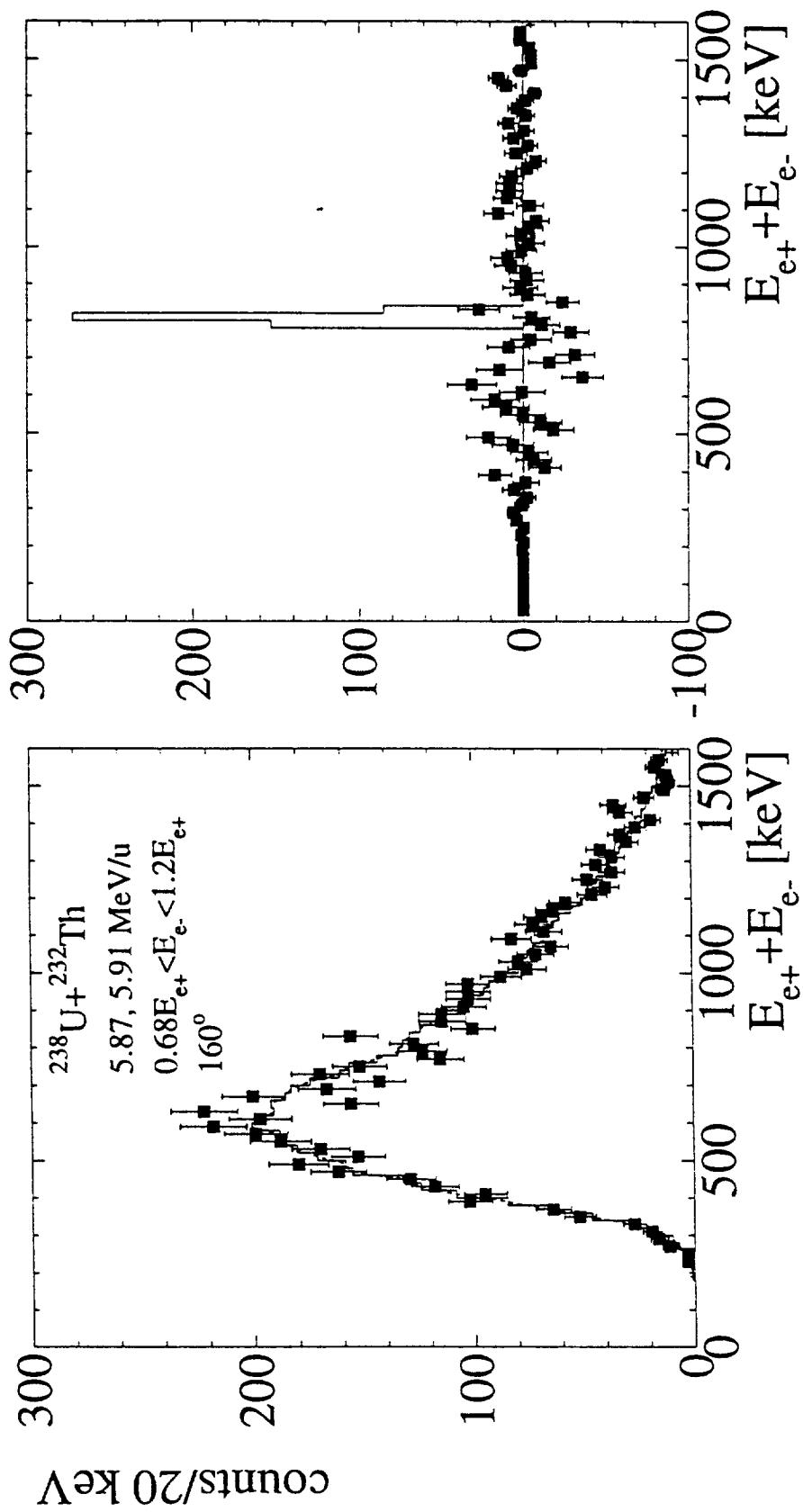


Figure 3:

